

# PARAMETERS OF SCALAR RESONANCES FROM THE COMBINED ANALYSIS OF DATA ON PROCESSES $\pi\pi \rightarrow \pi\pi, K\bar{K}, \eta\eta$ AND $J/\psi$ DECAYS

Yu.S. Surovtsev<sup>1</sup>, P. Bydžovský<sup>2</sup>, R. Kamiński<sup>3</sup>, V.E. Lyubovitskij<sup>4\*</sup>, and M. Nagy<sup>5</sup>

<sup>1</sup> *Bogoliubov Laboratory of Theoretical Physics,  
Joint Institute for Nuclear Research,  
141 980 Dubna, Russia*

<sup>2</sup> *Nuclear Physics Institute,  
Czech Academy of Sciences, 25068 Řež, Czech Republic*

<sup>3</sup> *Institute of Nuclear Physics,  
Polish Academy of Sciences, Cracow 31342, Poland*

<sup>4</sup> *Institut für Theoretische Physik, Universität Tübingen,  
Kepler Center for Astro and Particle Physics,  
Auf der Morgenstelle 14, D-72076 Tübingen, Germany*

<sup>5</sup> *Institute of Physics, Slovak Academy of Sciences,  
Bratislava 84511, Slovak Republic*

(Dated: June 4, 2019)

A combined analyses data on isoscalar S-wave processes  $\pi\pi \rightarrow \pi\pi, K\bar{K}, \eta\eta$  and on decays  $J/\psi \rightarrow \phi\pi\pi, \phi K\bar{K}$  from the DM2, Mark3 and BES collaborations is performed for studying  $f_0$ -mesons. The method of analysis is based on analyticity and unitarity and uses an uniformization procedure. In analysis only of the multi-channel  $\pi\pi$ -scattering, two possibilities were found for parameters of the  $f_0(600)$  with mass about 700 MeV and with total width about 600 and 930 MeV. The use of only DM2 and Mark3 data on the  $J/\psi$  decays does not permit to choose any of these possibilities. However the di-pion mass distribution in the decay  $J/\psi \rightarrow \phi\pi^+\pi^-$  from BES prefers clearly the wider  $f_0(600)$ . Some spectroscopic implications from results of the analysis are discussed.

PACS numbers: 11.55.Bq, 11.80.Gw, 12.39.Mk, 14.40.Cs

Keywords: coupled-channel formalism, meson-meson scattering, meson decays, scalar and pseudoscalar mesons

## I. INTRODUCTION

The comprehension of nature of  $f_0$  mesons is very important for such profound topics in particle physics as the QCD vacuum. However both parameters of the scalar mesons, obtained from experimental data in various analyses, and even the status of some of the mesons, are not quite definite [1, 2]. When discussing the first point, we pick out the  $f_0(600)/\sigma$ -meson,  $f_0(980)$  and  $f_0(1500)$ . As to the second point, one might indicate a situation related to the  $f_0(1370)$  when, e.g., D. Bugg [3] has indicated a number of data requiring apparently the existence of the  $f_0(1370)$ . These are the Crystal Barrel data on  $\bar{p}p \rightarrow \eta\eta\pi^0$  and on  $\bar{p}p \rightarrow 3\pi^0$  also the BES data on  $J/\psi \rightarrow \phi\pi^+\pi^-$ , and in the GAMS data for  $\pi^+\pi^- \rightarrow \pi^0\pi^0$  at large  $|t|$ . On the other hand, in works [4] one did not find evidence for the existence of the  $f_0(1370)$ . We have shown [2] that the existence of the  $f_0(1370)$  does not contradict the data on  $\pi\pi \rightarrow \pi\pi K\bar{K}, \eta\eta, \eta\eta'$ .

Note a situation with scalar states in the 1500-MeV region. In our previous model-independent analyses of  $\pi\pi \rightarrow \pi\pi K\bar{K}, \eta\eta(\eta\eta')$  we saw the wide state  $f_0(1500)$  whereas in works of some other authors, analyzing mainly mesons production and decay processes and cited in the PDG tables [1], the rather narrow  $f_0(1500)$  was obtained. We suggested that the wide  $f_0(1500)$ , observed in the multi-channel  $\pi\pi$  scattering, indeed, is a superposition of two states, wide and narrow. The latter is observed just in decays and productions of mesons. Here we verify also this suggestion.

---

\* On leave of absence from the Department of Physics, Tomsk State University, 634050 Tomsk, Russia

In view of indicated circumstances, related to parameters and status of scalar mesons, there are known problems as to determining their QCD nature and assignment to the quark-model configurations in spite of a big amount of work devoted these problems (see, e.g., [5] and references therein).

We present results of the combined coupled-channel analysis of data on isoscalar S-wave processes  $\pi\pi \rightarrow \pi\pi, K\bar{K}, \eta\eta$  and on decays  $J/\psi \rightarrow \pi\pi, K\bar{K}$  for studying  $f_0$ -mesons lying below 1.9 GeV. To analysis of experimental data we applied our model-independent method based only on the first principles (analyticity and unitarity) [6]. That approach permits us to omit theoretical prejudice in extracting the resonance parameters. Considering the obtained arrangement of resonance poles on the Riemann-surface sheets, obtained coupling constants with channels and resonance masses, we draw definite conclusions about nature of the investigated states.

## II. THE 3-COUPLED-CHANNEL FORMALISM IN MODEL-INDEPENDENT APPROACH WITH UNIFORMIZING VARIABLE

Our model-independent method which essentially utilizes an uniformizing variable can be used only for the 2-channel case and under some conditions for the 3-channel one. Only in these cases we obtain a simple symmetric (easily interpreted) picture of the resonance poles and zeros of the  $S$ -matrix on the uniformization plane. The 3-channel  $S$ -matrix is determined on the 8-sheeted Riemann surface. The matrix elements  $S_{ij}$ , where  $i, j = 1, 2, 3$  denote channels, have the right-hand cuts along the real axis of the  $s$  complex plane ( $s$  is the invariant total energy squared), starting with the channel thresholds  $s_i$  ( $i = 1, 2, 3$ ), and the left-hand cuts. The Riemann-surface sheets are numbered according to the signs of analytic continuations of the square roots  $\sqrt{s - s_i}$  ( $i = 1, 2, 3$ ) as follows: signs $(\text{Im}\sqrt{s - s_1}, \text{Im}\sqrt{s - s_2}, \text{Im}\sqrt{s - s_3}) = +++, -++, --, +-, +--, -, +-, +-$  correspond to sheets I, II,  $\dots$ , VIII, respectively.

The resonance representations on the Riemann surface are obtained with the help of formulas from [2, 6], expressing analytic continuations of the  $S$ -matrix elements to all sheets in terms of those on sheet I that have only the resonances zeros (beyond the real axis), at least, around the physical region:

TABLE I: Analytic continuations of the 3-channel  $S$ -matrix elements to unphysical sheets

Process	$1 \rightarrow 1$	$1 \rightarrow 2$	$2 \rightarrow 2$	$1 \rightarrow 3$	$2 \rightarrow 3$	$3 \rightarrow 3$
I	$S_{11}$	$S_{12}$	$S_{22}$	$S_{13}$	$S_{23}$	$S_{33}$
II	$1/S_{11}$	$iS_{12}/S_{11}$	$D_{33}/S_{11}$	$iS_{13}/S_{11}$	$D_{23}/S_{11}$	$D_{22}/S_{11}$
III	$S_{22}/D_{33}$	$-S_{12}/D_{33}$	$S_{11}/D_{33}$	$-iD_{13}/D_{33}$	$iD_{23}/D_{33}$	$\det S/D_{33}$
IV	$D_{33}/S_{22}$	$iS_{12}/S_{22}$	$1/S_{22}$	$-D_{13}/S_{22}$	$iS_{23}/S_{22}$	$D_{11}/S_{22}$
V	$\det S/D_{11}$	$iD_{12}/D_{11}$	$S_{33}/D_{11}$	$-iD_{13}/D_{11}$	$-S_{23}/D_{11}$	$S_{22}/D_{11}$
VI	$D_{11}/\det S$	$-D_{12}/\det S$	$D_{22}/\det S$	$D_{13}/\det S$	$-D_{23}/\det S$	$D_{33}/\det S$
VII	$S_{33}/D_{22}$	$iD_{12}/D_{22}$	$\det S/D_{22}$	$-S_{13}/D_{22}$	$iD_{23}/D_{22}$	$S_{11}/D_{22}$
VIII	$D_{22}/S_{33}$	$D_{12}/S_{33}$	$D_{11}/S_{33}$	$iS_{13}/S_{33}$	$iS_{23}/S_{33}$	$1/S_{33}$

In Table I, the superscript  $I$  is omitted to simplify the notation,  $\det S$  is the determinant of the  $3 \times 3$   $S$ -matrix on sheet I,  $D_{\alpha\beta}$  is the minor of the element  $S_{\alpha\beta}$ , that is,  $D_{11} = S_{22}S_{33} - S_{23}^2$ ,  $D_{22} = S_{11}S_{33} - S_{13}^2$ ,  $D_{33} = S_{11}S_{22} - S_{12}^2$ ,  $D_{12} = S_{12}S_{33} - S_{13}S_{23}$ ,  $D_{23} = S_{11}S_{23} - S_{12}S_{13}$ , etc.

Then, starting from the resonance zeros on sheet I, one can obtain an arrangement of poles and zeros of resonance on the whole Riemann surface.

In the 3-channel case, we obtain 7 types of resonances corresponding to 7 possible situations when there are resonance zeros on sheet I only in  $S_{11}$  – (a);  $S_{22}$  – (b);  $S_{33}$  – (c);  $S_{11}$  and  $S_{22}$  – (d);  $S_{22}$  and  $S_{33}$  – (e);  $S_{11}$  and  $S_{33}$  – (f);  $S_{11}$ ,  $S_{22}$ , and  $S_{33}$  – (g).

The resonance of every type is represented by the pair of complex-conjugate clusters (of poles and zeros on the Riemann surface). A necessary and sufficient condition for existence of the multi-channel resonance is its representation by one of the types of pole clusters. Whereas cases (a), (b) and (c) can be related to the resonance representation by Breit-Wigner forms, cases (d), (e), (f) and (g) practically are lost at the Breit – Wigner description.

The cluster type is related to the nature of state. E.g., if we consider the  $\pi\pi, K\bar{K}$  and  $\eta\eta$  channels, then a resonance, coupled relatively more strongly to the  $\pi\pi$  channel than to the  $K\bar{K}$  and  $\eta\eta$  ones is described by the cluster of type (a). In the opposite case, it is represented by the cluster of type (e) (say, the state with the dominant  $s\bar{s}$  component). The glueball must be represented by the cluster of type (g) as a necessary condition for the ideal case.

From formulas of the analytic continuations, we conclude that parameters of resonances (masses, total widths and coupling constants with channels) must be calculated using the pole positions on sheets II, IV and VIII because the analytic continuations only onto these sheets have the forms:  $\propto 1/S_{11}^I$ ,  $\propto 1/S_{22}^I$  and  $\propto 1/S_{33}^I$ , respectively, i.e., the pole positions of resonances only on these sheets are at the same points of the complex-energy plane, as the resonance zeros on the physical sheet, and are not shifted due to the coupling of channels.

One can distinguish [6, 7], in a model-independent way, a bound state of colourless particles (*e.g.*,  $K\bar{K}$  molecule) and a  $q\bar{q}$  bound state. Just as in the 1-channel case, the existence of the particle bound-state means the presence of a pole on the real axis under the threshold on the physical sheet, so in the 2-channel case, the existence of the bound-state in channel 2 ( $K\bar{K}$  molecule) that, however, can decay into channel 1 ( $\pi\pi$  decay), would imply the presence of the pair of complex conjugate poles on sheet II under the second-channel threshold without the corresponding shifted pair of poles on sheet III. In the 3-channel case, the bound state in channel 3 ( $\eta\eta$ ) that, however, can decay into channels 1 ( $\pi\pi$  decay) and 2 ( $K\bar{K}$  decay), is represented by the pair of complex conjugate poles on sheet II and by the pair of shifted poles on sheet III under the  $\eta\eta$  threshold without the corresponding poles on sheets VI and VII.

It is convenient to use the Le Couteur-Newton relations [8]. They express the  $S$ -matrix elements of all coupled processes in terms of the Jost matrix determinant  $d(\sqrt{s} - s_1, \dots, \sqrt{s} - s_n)$  that is a real analytic function with the only square-root branch-points at  $\sqrt{s} - s_i = 0$ . The important branch points, corresponding to the thresholds of the coupled channels and to the crossing ones, are taken into account in the proper uniformizing variable. Here we used an uniformizing variable, in which we neglect the lowest  $\pi\pi$ -threshold branch-point and take into account the threshold branch-points related to two remaining channels and the left-hand branch-point at  $s = 0$  [2]:

$$w = \frac{\sqrt{(s - s_2)s_3} + \sqrt{(s - s_3)s_2}}{\sqrt{s(s_3 - s_2)}}, \quad (1)$$

here  $s_2 = m_K^2$ ,  $s_3 = 4m_\eta^2$ . It maps our model of the 8-sheeted Riemann surface onto the uniformization  $w$ -plane. On Figs. II resonances of the **(a)**, **(b)**, **(c)** and **(g)** types, met in this analysis, are represented in  $S_{11}$  by the poles (\*) and zeros (○) symmetric to these poles with respect to the imaginary axis. The Roman numerals denote images of the corresponding sheets of the Riemann surface; the thick line represents the physical region; the points  $\pi\pi$ ,  $i$ , 1 and  $b = (\sqrt{s_3} + \sqrt{s_2})/\sqrt{s_3 - s_2}$  correspond to the  $\pi\pi$ ,  $K\bar{K}$ ,  $\eta\eta$  thresholds and  $s = \infty$ , respectively; the shaded intervals  $(-\infty, -b]$ ,  $[-b^{-1}, b^{-1}]$ ,  $[b, \infty)$  are the images of the corresponding edges of the left-hand cut of the  $\pi\pi$ -scattering amplitude.

On the  $w$ -plane, the Le Couteur-Newton relations are [6]:

$$\begin{aligned} S_{11} &= \frac{d^*(-w^*)}{d(w)}, & S_{22} &= \frac{d(-w^{-1})}{d(w)}, & S_{33} &= \frac{d(w^{-1})}{d(w)}, \\ S_{11}S_{22} - S_{12}^2 &= \frac{d^*(w^{*-1})}{d(w)}, & S_{11}S_{33} - S_{13}^2 &= \frac{d^*(-w^{*-1})}{d(w)}. \end{aligned} \quad (2)$$

The main model-independent effect of multi-channel resonances is given by the pole clusters. Assuming that possible remaining small (model-dependent) contributions of resonances can be included via the background, the  $S$ -matrix elements are taken as the products

$$S = S_B S_{res} \quad (3)$$

where  $S_B$  describes the background,  $S_{res}$  the resonance contributions. The  $d$ -function for resonance part is

$$d_{res}(w) = w^{-\frac{M}{2}} \prod_{r=1}^M (w + w_r^*) \quad (4)$$

with  $M$  the number of resonance zeros. For the background part  $S_B$ , the  $d$ -function has the following form:

$$d_B = \exp[-i(a + \sum_{n=1}^3 \frac{\sqrt{s - s_n}}{2m_n} (\alpha_n + i\beta_n))] \quad (5)$$

where

$$\begin{aligned} \alpha_n &= a_{n1} + a_{n\sigma} \frac{s - s_\sigma}{s_\sigma} \theta(s - s_\sigma) + a_{nv} \frac{s - s_v}{s_v} \theta(s - s_v), \\ \beta_n &= b_{n1} + b_{n\sigma} \frac{s - s_\sigma}{s_\sigma} \theta(s - s_\sigma) + b_{nv} \frac{s - s_v}{s_v} \theta(s - s_v) \end{aligned} \quad (6)$$

with  $s_\sigma$  the  $\sigma\sigma$  threshold,  $s_v$  the combined threshold of many opening channels in the range of  $\sim 1.5$  GeV ( $\eta\eta'$ ,  $\rho\rho$ ,  $\omega\omega$ ). These threshold are determined in the analysis.

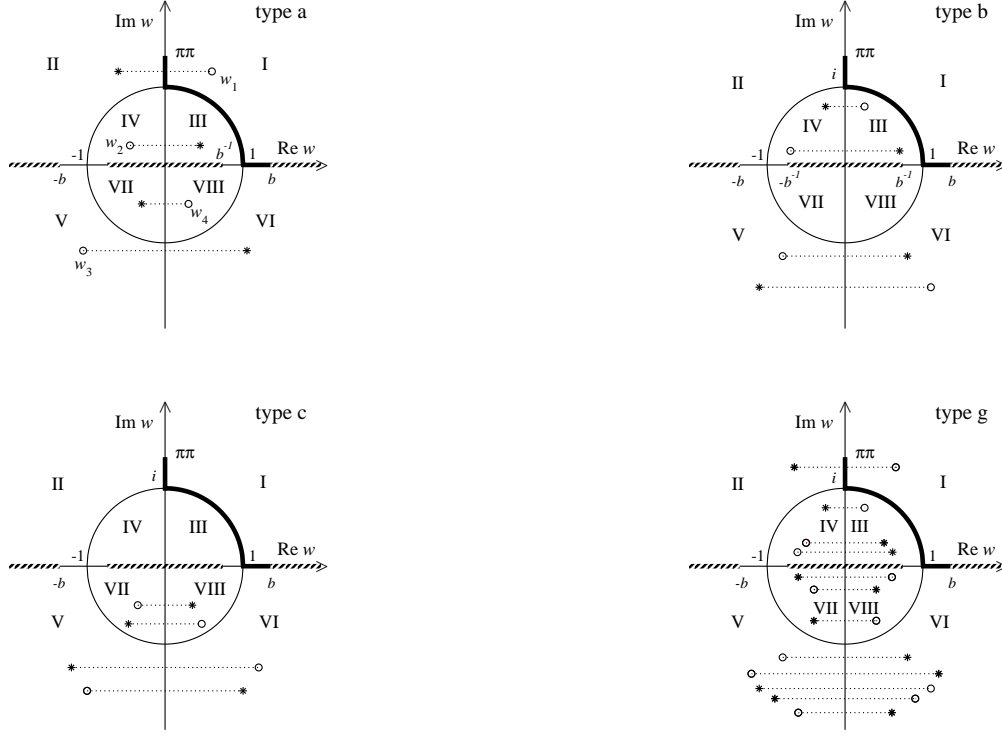


FIG. 1: Uniformization  $w$ -plane: Representation of resonances of types (a), (b), (c) and (g) in the 3-channel  $\pi\pi$ -scattering  $S$ -matrix element.

### III. ANALYSIS OF THE DATA ON ISOSCALAR S-WAVE PROCESSES $\pi\pi \rightarrow \pi\pi, K\bar{K}, \eta\eta$ AND ON DECAYS $J/\psi \rightarrow \phi\pi\pi, \phi K\bar{K}$

In the combined analysis of data on processes  $\pi\pi \rightarrow \pi\pi, K\bar{K}, \eta\eta$  (references to used data are in [2]) we added also data on decays  $J/\psi \rightarrow \phi\pi\pi, \phi K\bar{K}$  from Mark III [9], DM2 [10] and BES [11] collaborations. Formalism for calculating di-meson mass distributions of these decays can be found in Refs. [7, 12]. There it is assumed that the pairs of the pseudo-scalar mesons of the final states have  $I = J = 0$  and that only these pairs undergo strong interactions, whereas the  $\phi$  meson acts as a spectator.

The amplitudes for  $J/\psi \rightarrow \phi\pi\pi, \phi K\bar{K}$  decays are related with the scattering amplitudes  $T_{ij}$   $i, j = 1 - \pi\pi, 2 - K\bar{K}$  as follows

$$F(J/\psi \rightarrow \phi\pi\pi) = \sqrt{2/3} [c_1(s)T_{11} + c_2(s)T_{21}], \quad (7)$$

$$F(J/\psi \rightarrow \phi K\bar{K}) = \sqrt{1/2} [c_1(s)T_{12} + c_2(s)T_{22}], \quad (8)$$

where  $c_i = \alpha_i/(s - \beta_i) + \gamma_{i0} + \gamma_{i1}s$  are functions of couplings of the  $J/\psi$  to channel  $i$ ;  $\alpha_i, \beta_i, \gamma_{i0}$  and  $\gamma_{i1}$  are free parameters. The first term in  $c_i$  is related to the on-shell manifestation of Adler zero. The di-meson mass distributions are given as

$$N|F|^2 \sqrt{(s - s_i)(m_\psi^2 - (\sqrt{s} - m_\phi)^2)(m_\psi^2 - (\sqrt{s} + m_\phi)^2)} \quad (9)$$

where  $N$  (normalization to experiment) is 0.725 for Mark III, 0.347 for DM2 and 5.653 for BES data (from analysis). Parameters of the  $c_i$ -functions, obtained in the analysis, are  $\alpha_1, \beta_1 \alpha_2, \beta_2 = 0.0306, 0.0646, 0.0222, 0.0701$  and  $\gamma_{10}, \gamma_{11}, \gamma_{20}, \gamma_{21} = 1.1902, 1.3622, -1.2823, -1.6748$ .

In the analysis we supposed that in the 1500-MeV region there are two resonances: the narrow  $f_0(1500)$  and wide  $f'_0(1500)$ . From the analysis, the  $f_0(600)$  is described by the cluster of type (a);  $f_0(1500)$ , type (c) and  $f'_0(1500)$ , type

(g); the  $f_0(980)$  is represented only by the pole on sheet II and shifted pole on sheet III. However, for representation of the  $f_0(1370)$  and  $f_0(1710)$ , there are some possibilities. These states are described by clusters either of type (b) or type (c). Analyzing only the processes  $\pi\pi \rightarrow \pi\pi, K\bar{K}, \eta\eta, \eta\eta'$  [2], it is impossible to prefer surely any of four indicated possibilities; moreover, it was found that the data admit two possibilities for parameters of the  $f_0(600)$  with mass, relatively near to the  $\rho$ -meson mass, and with the total widths about 600 and 950 MeV.

When adding to the combined analysis, the data on decays  $J/\psi \rightarrow \phi\pi\pi, \phi K\bar{K}$ , one can give some preference for scenarios when the  $f_0(1370)$  is described by the cluster of type (b),  $f_0(1710)$  either of type (b) or (c). Further, for definiteness, we shall tell about the case when the  $f_0(1710)$  is represented by the cluster of type (c).

It is interesting that the di-pion mass distribution of the  $J/\psi \rightarrow \phi\pi\pi$  decay of the BES data from the threshold to about 0.85 GeV prefers surely the solution with the more wide  $f_0(600)$ . Satisfactory combined description of all analyzed processes is obtained with the total  $\chi^2/NDF = 424.317/(389 - 55) \approx 1.26$ ; for the  $\pi\pi$  scattering,  $\chi^2/NDF \approx 1.20$ ; for  $\pi\pi \rightarrow K\bar{K}$ ,  $\chi^2/NDF \approx 1.64$ ; for  $\pi\pi \rightarrow \eta\eta$ ,  $\chi^2/ndp \approx 0.82$ ; for decays  $J/\psi \rightarrow \phi\pi\pi, \phi K\bar{K}$ ,  $\chi^2/NDF \approx 1.55$ .

Figures 2–6 demonstrate the fitting to experimental data.

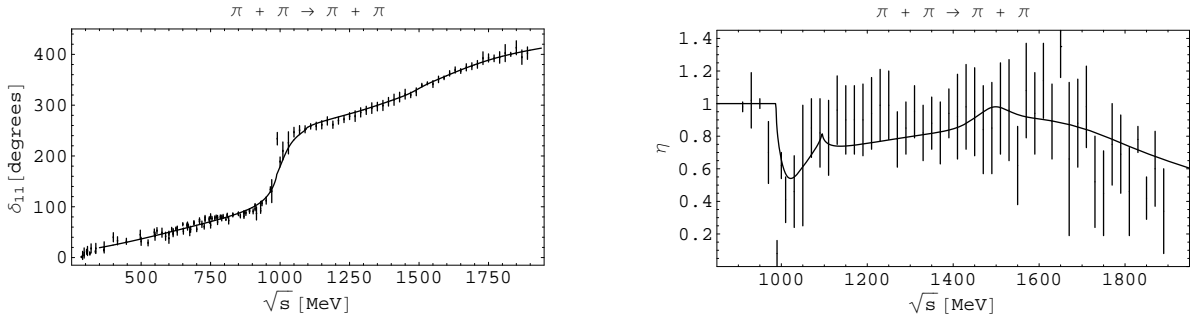


FIG. 2: The phase shift and module of the  $\pi\pi$ -scattering  $S$ -wave matrix element.

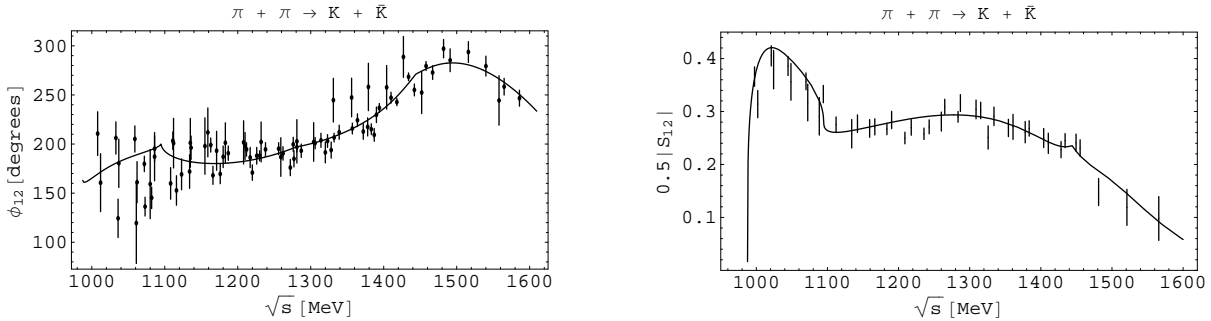


FIG. 3: The phase shift and module of the  $\pi\pi \rightarrow K\bar{K}$   $S$ -wave matrix element.

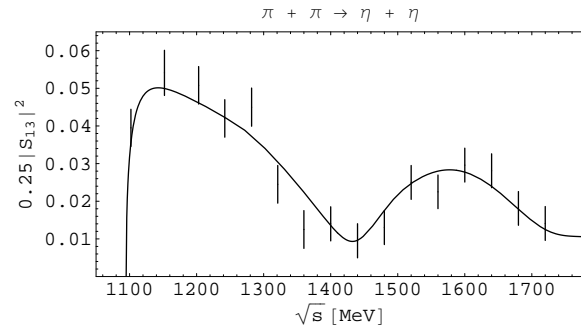


FIG. 4: The squared modules of the  $\pi\pi \rightarrow \eta\eta$   $S$ -wave matrix element.

In Table II we show the obtained pole clusters for the resonances in the complex energy plane  $\sqrt{s}$ ; the poles on sheets IV, VI, VIII and V, corresponding to the  $f_0'(1500)$ , are of the 2nd and 3rd order, respectively (this is an approximation).

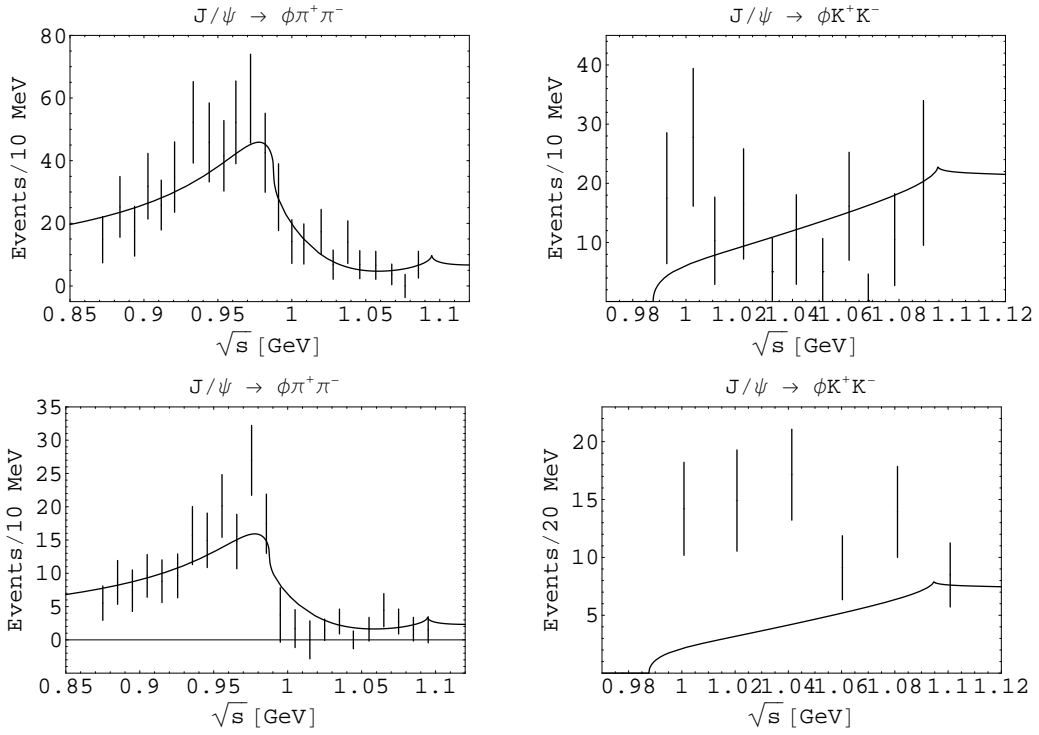


FIG. 5: The  $J/\psi \rightarrow \phi\pi\pi, \phi K\bar{K}$  decays. The upper panel shows the fit to data of Mark III, the lower to DM2.

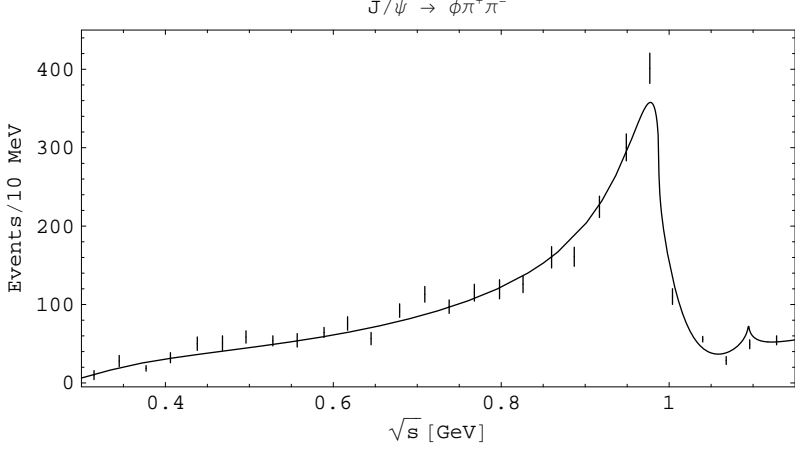


FIG. 6: The  $J/\psi \rightarrow \phi\pi\pi$  decay; the data of BES Collaboration.

The obtained background parameters are:  $a = a_{11} = 0.0, a_{1\sigma} = 0.0198, a_{1v} = 0.0, b_{11} = b_{1\sigma} = 0.0, b_{1v} = 0.0336, a_{21} = -2.4808, a_{2\sigma} = -2.3021, a_{2v} = -6.62, b_{21} = b_{2\sigma} = 0.0, b_{2v} = 6.99, b_{31} = 0.6432, b_{3\sigma} = 0.489, b_{2v} = 0; s_\sigma = 1.6384 \text{ GeV}^2, s_v = 2.0851 \text{ GeV}^2$ .

The obtained very simple description of the  $\pi\pi$ -scattering background confirms well our assumption (3).

Generally, wide multi-channel states are most adequately represented by pole clusters, because the pole clusters give a main model-independent effect of resonances. The pole positions are rather stable characteristics for various models, whereas masses and widths are very model-dependent for wide resonances. However, mass values are needed in some case, e.g., in mass relations for multiplets. Therefore, we stress that they should be calculated using the poles on sheets II, IV, VIII, depending on the resonance classification. E.g., if

$$T^{res} = \sqrt{s} \Gamma_{el} / (m_{res}^2 - s - i\sqrt{s} \Gamma_{tot}),$$

TABLE II: The pole clusters for resonances on the  $\sqrt{s}$ -plane.  $\sqrt{s_r} = E_r - i\Gamma_r/2$ .

Sheet		$f_0(600)$	$f_0(980)$	$f_0(1370)$	$f_0(1500)$	$f'_0(1500)$	$f_0(1710)$
II	$E_r$	$521.6 \pm 12.4$	$1008.4 \pm 3.1$			$1512.4 \pm 4.9$	
	$\Gamma_r/2$	$467.3 \pm 5.9$	$33.5 \pm 1.5$			$287.2 \pm 12.9$	
III	$E_r$	$552.5 \pm 17.7$	$976.7 \pm 5.8$	$1387.2 \pm 24.4$		$1506.1 \pm 9.0$	
	$\Gamma_r/2$	$467.3 \pm 5.9$	$53.2 \pm 2.6$	$167.2 \pm 41.8$		$127.8 \pm 10.6$	
IV	$E_r$			$1387.2 \pm 24.4$		$1512.4 \pm 4.9$	
	$\Gamma_r/2$			$178.2 \pm 37.2$		$215.0 \pm 17.6$	
V	$E_r$			$1387.2 \pm 24.4$	$1493.9 \pm 3.1$	$1498.8 \pm 7.2$	$1732.8 \pm 43.2$
	$\Gamma_r/2$			$261.0 \pm 73.7$	$72.8 \pm 3.9$	$142.3 \pm 6.0$	$114.8 \pm 61.5$
VI	$E_r$	$573.4 \pm 29.1$		$1387.2 \pm 24.4$	$1493.9 \pm 5.6$	$1511.5 \pm 4.3$	$1732.8 \pm 43.2$
	$\Gamma_r/2$	$467.3 \pm 5.9$		$250.0 \pm 83.1$	$58.4 \pm 2.8$	$179.3 \pm 4.0$	$111.2 \pm 8.8$
VII	$E_r$	$542.5 \pm 25.5$			$1493.9 \pm 5.0$	$1500.4 \pm 9.3$	$1732.8 \pm 43.2$
	$\Gamma_r/2$	$467.3 \pm 5.9$			$47.8 \pm 9.3$	$99.9 \pm 18.0$	$55.2 \pm 38.0$
VIII	$E_r$				$1493.9 \pm 3.2$	$1512.4 \pm 4.9$	$1732.8 \pm 43.2$
	$\Gamma_r/2$				$62.2 \pm 9.2$	$298.4 \pm 14.5$	$58.8 \pm 16.4$

$$m_{res} = \sqrt{E_r^2 + (\Gamma_r/2)^2} \quad \text{and} \quad \Gamma_{tot} = \Gamma_r.$$

In Table III we show the obtained masses and widths for the  $f_0$  states.

TABLE III: Masses and total widths of the  $f_0$  states.

	$f_0(600)$	$f_0(980)$	$f_0(1370)$	$f_0(1500)$	$f'_0(1500)$	$f_0(1710)$
$m_{res} [\text{MeV}]$	$700.3 \pm 10.0$	$1009.0 \pm 3.1$	$1398.6 \pm 24.7$	$1495.2 \pm 3.2$	$1539.4 \pm 5.4$	$1733.8 \pm 43.2$
$\Gamma_{tot} [\text{MeV}]$	$934.6 \pm 11.8$	$67.0 \pm 3.0$	$356.4 \pm 74.4$	$124.4 \pm 18.4$	$574.4 \pm 25.8$	$117.6 \pm 32.8$

#### IV. DISCUSSION AND CONCLUSIONS

- In the combined model-independent analysis of data on  $\pi\pi \rightarrow \pi\pi, K\bar{K}, \eta\eta$  in the  $I^G J^{PC} = 0^+ 0^{++}$  channel and on  $J/\psi \rightarrow \phi\pi\pi, \phi K\bar{K}$  from Mark III, DM2 and BES collaborations, an additional confirmation of the  $f_0(600)$  with mass about 700 MeV and width 930 MeV is obtained. This mass value accords with prediction ( $m_\sigma \approx m_\rho$ ) on the basis of mended symmetry by Weinberg [14]. This is also in agreement with a refined analysis using the large- $N_c$  consistency conditions between the unitarization and resonance saturation suggesting  $m_\rho - m_\sigma = O(N_c^{-1})$  [15].
- Indication for  $f_0(980)$  ( $m_{res} = 1009$  MeV,  $\Gamma_{tot} = 67$  MeV) is obtained to be, e.g., the bound  $\eta\eta$  state, because this state lies slightly above the  $K\bar{K}$  threshold and is described by the pole on sheet II and by the shifted pole on sheet III without the corresponding (for standard clusters) poles on sheets VI and VII.
- The  $f_0(1370)$  and  $f_0(1710)$  have the dominant  $s\bar{s}$  component. Conclusion about the  $f_0(1370)$  quite agrees with the one of work of Crystal Barrel Collaboration [16] where the  $f_0(1370)$  is identified as  $\eta\eta$  resonance in the  $\pi^0\eta\eta$  final state of the  $\bar{p}p$  annihilation at rest. This explains also quite well why one did not find this state considering only the  $\pi\pi$  scattering [4]. Conclusion about the  $f_0(1710)$  is consistent with the experimental facts that this state is observed in  $\gamma\gamma \rightarrow K_SK_S$  [17] and not observed in  $\gamma\gamma \rightarrow \pi^+\pi^-$  [18].
- In the 1500-MeV region, indeed, there are two states: the  $f_0(1500)$  ( $m_{res} \approx 1495$  MeV,  $\Gamma_{tot} \approx 124$  MeV) and the  $f'_0(1500)$  ( $m_{res} \approx 1539$  MeV,  $\Gamma_{tot} \approx 574$  MeV). The  $f'_0(1500)$  is interpreted as a glueball taking into account its biggest width among enclosing states [19].

- We propose the following assignment of the scalar mesons to lower nonets, when excluding the  $f_0(980)$  as the non- $q\bar{q}$  state. The lowest nonet: the isovector  $a_0(980)$ , the isodoublet  $K_0^*(800)$ , and  $f_0(600)$  and  $f_0(1370)$  as mixtures of the 8th component of octet and the SU(3) singlet. The Gell-Mann–Okubo (GM-O) formula

$$3m_{f_8}^2 = 4m_{K_0^*}^2 - m_{a_0}^2$$

gives  $m_{f_8} = 870$  MeV.

In relation for masses of nonet

$$m_\sigma + m_{f_0(1370)} = 2m_{K_0^*}$$

the left-hand side is by about 17% bigger than the right-hand one.

- For the next nonet we find: the isovector  $a_0(1450)$ , the isodoublet  $K_0^*(1450)$ , and two isoscalars  $f_0(1500)$  and  $f_0(1710)$ . From the GM-O formula,  $m_{f_8} \approx 1450$  MeV. In formula

$$m_{f_0(1500)} + m_{f_0(1710)} = 2m_{K_0^*(1450)}$$

the left-hand side is by about 11% bigger than the right-hand one.

- This assignment removes a number of questions, stood earlier, and does not put any new. The mass formulas indicate to non-simple mixing scheme. The breaking of 2nd mass relations tells us that the  $\sigma - f_0(1370)$  and  $f_0(1500) - f_0(1710)$  systems get additional contributions absent in the  $K_0^*(900)$  and  $K_0^*(1450)$ , respectively. A search of the adequate mixing scheme is complicated by the fact that here there is also a remainder chiral symmetry, though, on the other hand, this permits one to predict correctly, *e.g.*, the  $\sigma$ -meson mass [14].

### Acknowledgements

This work was supported in part by the Heisenberg–Landau Program, the RFBR grant 10-02-00368-a, the Votruba–Blokhintsev Program for Cooperation of Czech Republic with JINR, the Grant Program of Plenipotentiary of Slovak Republic at JINR, the Bogoliubov–Infeld Program for Cooperation of Poland with JINR, the Polish Ministry of Science and Higher Education (grant No N N202 101 368).

---

[1] K. Nakamura *et al.* (PDG), J. Phys. **G37** (2010) 075021.  
[2] Yu.S. Surovtsev, P. Bydžovský and V.E. Lyubovitskij, Phys. Rev. **D85** (2012) 036002.  
[3] D. Bugg, Eur. Phys. J. **C52** (2007) 55; arXiv: 0710.4452 [hep-ex].  
[4] W. Ochs, arXiv:1001.4486v1 [hep-ph]; P. Minkowski and W. Ochs, Eur. Phys. J. **C9** (1999) 283; arXiv: hep-ph/0209223; hep-ph/0209225.  
[5] V.V. Anisovich, Int. J. Mod. Phys. **A21** (2006) 3615.  
[6] D. Krupa, V.A. Meshcheryakov and Yu.S. Surovtsev, Nuovo Cim. **A109** (1996) 281.  
[7] D. Morgan and M.R. Pennington, Phys. Rev. **D48** (1993) 1185, 5422.  
[8] K.J. Le Couteur, Proc. R. London, Ser. A **256** (1960) 115; R.G. Newton, J. Math. Phys. **2** (1961) 188; M. Kato, Ann. Phys. **31** (1965) 130.  
[9] W. Lockman, Proceedings of the Hadron'89 Conference, ed. F. Binon *et al.* (Editions Frontières, Gif-sur-Yvette, 1989) p.109.  
[10] A. Falvard *et al.*, Phys. Rev. **D38** (1988) 2706.  
[11] M. Ablikim *et al.*, Phys. Lett. **B607** (2005) 243.  
[12] B.S. Zou and D.V. Bugg, Phys. Rev. **D50** (1994) 591.  
[13] Yu.S. Surovtsev, P. Bydžovský, R. Kamiński, V.E. Lyubovitskij, and M. Nagy, arXiv: 1206.3438v2 [hep-ph].  
[14] S. Weinberg, Phys. Rev. Lett. **65** (1990) 1177.  
[15] J. Nieves and E. Ruiz Arriola, Phys. Rev. **D80** (2009) 045023.  
[16] C. Amsler *et al.*, Phys. Lett. **B355** (1995) 425.  
[17] S. Braccini, Frascati Phys. Series **XV** (1999) 53.  
[18] R. Barate *et al.*, Phys. Lett. **B472** (2000) 189.  
[19] V.V. Anisovich *et al.*, Nucl. Phys. Proc. Suppl. **A56** (1997) 270.